Journal of Nuclear and Particle Physics 2014, 4(3): 94-99
DOI: 10.5923/j.jnpp.20140403.02

Semi-empirical Evaluation of the Plasma Internal Inductance in Tokamaks

A. Paknezhad[1,*], A. Salar Elahi[2], M. Ghoranneviss[2]

[1]Physics Department, Shabestar Branch-Islamic Azad University, Shabestar, Iran
[2]Plasma Physics Research Center, Science and Research Branch, Islamic Azad University, Tehran, Iran

Abstract In this paper we presented an analytical and experimental approach for measurement of the plasma internal inductance in IR-T1 tokamak. For this purpose, a diamagnetic loop with its compensation coil, and also an array of magnetic probes were designed, constructed, and installed on outer surface of the IR-T1 tokamak chamber, and the poloidal beta and the Shafranov parameter and then the internal inductance measured. Moreover, a few approximate values of the internal inductance for different possible profiles of the plasma current density are also calculated.

Keywords Tokamak, Plasma Internal Inductance, Diamagnetic Loop, Magnetic Probe

1. Introduction

Because of the relation between the plasma internal inductance and plasma current profile, it is one of the main parameters of the tokamak plasma. Magnetic diagnostics, in particular toroidal flux loop (diamagnetic loop) are commonly used in tokamaks to measure the variation of toroidal flux induced by the plasma. From this measurement, the total diamagnetic energy content and the confinement time of the plasma can be obtained as well as the poloidal beta. On the other hand, measurements of the magnetic fields distribution outside the plasma give us the Shafranov parameter (asymmetry factor $\Lambda = \beta_p + l_i / 2 - 1$). Therefore, the plasma internal inductance is can be obtained using subtraction. Also the value of l_i is determined by the radial distribution of toroidal current profile of the plasma [1-13].

In this paper we presented an experimental approach based on the diamagnetic loop and magnetic probe, and moreover an approximate calculations for determination of the plasma internal inductance in IR-T1 Tokamak, which is a small, low β_p and large aspect ratio tokamak with a circular cross section (see Table 1) [14-67]. Details of the experimental approach for measurement of the plasma internal inductance will be presented in section 2. Details of approximate calculations for determination of the internal inductance will be presented in section 3. Experimental results will be discussed in section 4. Also summary will be presented in section 5.

Table 1. Main parameters of the IR-T1 tokamak

Parameters	Value
Major Radius	45 cm
Minor Radius	12.5 cm
Toroidal Field	$\langle$ 1.0 T
Plasma Current	$\langle$ 40 kA
Discharge Time	$\langle$ 35 ms
Electron Density	0.7-1.5 $\times 10^{13}$ cm^{-3}

2. Experimental Approach for Measurement of the Plasma Internal Inductance

Shafranov parameter relate to the distribution of magnetic fields around the plasma current. Therefore, it can be written in terms of the tangential and normal components of the magnetic field around the plasma. Distributions of the poloidal and radial magnetic fields are can be written in the first order of the inverse aspect ratio as follows, respectively [1]:

$$B_\theta = \frac{\mu_0 I_p}{2\pi \mathrm{b}} - \frac{\mu_0 I_p}{4\pi R_0} \times \left\{ \ln\frac{a}{b} + 1 - \left(\Lambda + \frac{1}{2}\right)\left(\frac{a^2}{b^2} + 1\right) - \frac{2R_0\Delta_s}{b^2} \right\} \cos\theta, \quad (1)$$

* Corresponding author:
A.Paknezhad@iaushab.ac.ir (A. Paknezhad)
Published online at http://journal.sapub.org/jnpp

$$B_r = -\frac{\mu_0 I_p}{4\pi R_0} \times \left\{ \ln\frac{a}{b} + \left(\Lambda + \frac{1}{2}\right)\left(\frac{a^2}{b^2} - 1\right) + \frac{2R_0\Delta_s}{b^2} \right\} \sin\theta, \quad (2)$$

where R_0 is the major radius of the vacuum vessel, Δ_s is the Shafranov shift, I_p is the plasma current, a and b are the minor plasma radius and minor chamber radius respectively, and Λ is the Shafranov parameter. These equations accurate for low β plasma and circular cross section tokamaks as IR-T1, and where:

$$\Lambda = \beta_p + l_i / 2 - 1, \quad (3)$$

where β_p is the poloidal beta, and l_i is the plasma internal inductance.

Rearranging of the Eq. (3) give us the first relation for l_i:

$$l_{i1} = 2(\Lambda - \beta_p + 1). \quad (4)$$

Also by rearranging and combination of the Eq. (1) and Eq. (2) the Shafranov parameter can be measured:

$$\Lambda = \ln\frac{a}{b} + \frac{\pi R_0}{\mu_0 I_0}(\langle B_\theta \rangle + \langle B_n \rangle),$$
$$\textit{where}$$
$$\langle B_\theta \rangle = B_\theta(\theta = 0) - B_\theta(\theta = \pi), \quad (5)$$
$$\langle B_n \rangle = B_n(\theta = \frac{\pi}{2}) - B_n(\theta = \frac{3\pi}{2}),$$

which can be measured using the magnetic probes. Also the poloidal beta is can be measured using the diamagnetic loop. Therefore, with combination of the magnetic probes and diamagnetic loop measurements, the internal inductance can be measured from the Eq. (4).

Magnetic probes consist of a coil in solenoidal form, which whose dimensions are small compared to the gradient scale length of the magnetic field. A total magnetic flux passed through such a coil is $\Phi_B = nAB$, where n is the number of turns of coil, A is the average area of cross section of coil, and B is the local magnetic field parallel to the coil axis.

The induced voltage in the magnetic probe and then magnetic field is:

$$|V_i| = \frac{d\Phi_B}{dt} = nA\frac{dB}{dt} = nA\,\omega\,B,$$
$$B = \frac{1}{nA}\int V_i dt, \quad (6)$$

where ω is the frequency of the fluctuations of the magnetic field. Therefore in order to measurement of the magnetic field distribution we must be integrating the output signals of the magnetic probe.

On the other hand, diamagnetic loop measures the toroidal diamagnetic flux for the purpose of measurement of the poloidal beta and thermal energy of the plasma. It is usually a single wire which circling the plasma column either inside or outside of the plasma vacuum chamber. Intrinsically this loop will also pickup the toroidal magnetic flux from the toroidal field coil and any current circulating in the poloidal plane, in particular toroidal field coil current, eddy currents in the conducting vacuum chamber induced during transient changes in the plasma energy and plasma current. In other words, the diamagnetic loop consist of a simple loop that links the plasma column, ideally located in a poloidal direction in order to minimize detecting the poloidal field. Relation between the diamagnetic flux and the poloidal beta derived from simplified equilibrium relation [2-4] is:

$$\beta_p = 1 - \frac{8\pi\,\mathrm{B}_{\phi 0}}{\mu_0^2 I_p^2}\Delta\Phi_D, \quad (7)$$

where $\Delta\Phi_D = \Phi_{total} - \Phi_{vacuum}$,

and where $\Phi_{vacuum} = \Phi_T + \Phi_O + \Phi_V + \Phi_E$,

where $B_{\phi 0}$ is the toroidal magnetic field in the absence of the plasma which can be obtained by the magnetic probe or diamagnetic loop, I_p is the plasma current which can be obtained by the rogowski coil, Φ_T is the toroidal flux because of toroidal field coils, Φ_O and Φ_V are the passing flux through loop due to possible misalignment between ohmic field and vertical field and the diamagnetic loop and Φ_E is the toroidal field due to eddy current on the vacuum chamber. These fluxes can be compensated either with compensation coil or dry runs technique. It must be noted that compensating coil for diamagnetic loop is wrapped out of the plasma current, and only the toroidal flux (which is induced by the change of toroidal field coil current when plasma discharges) can be received.

According to above discussion, we designed, constructed, and installed four magnetic probes and also diamagnetic loop with its compensation coil, on outer surface of the IR-T1, in order to measurements of the Shafranov parameter and poloidal beta, respectively. Plasma current is also measured with Rogowski coil. Experimental results will be presented in the section 4.

3. Approximate Calculations of the Plasma Internal Inductance

The internal inductance of the plasma per unit length, normalized to $\mu_0 / 4\pi$ can be determined from the conservation of zeroth order magnetic energy:

$$l_i = \frac{L_i / 2\pi R_0}{\mu_0 / 4\pi} = \frac{2}{\mu_0^2 I_p^2 R_0} \int_{Plasma} B_\theta^2(r) d^3V \qquad (8)$$

For typical profile of the poloidal field which correspond to flat current density profile J_0 (usually accurate for low beta tokamak), as:

$$\begin{cases} J = J_0 \rightarrow B_\theta = B_{\theta\, a} \dfrac{r}{a} & \mathrm{r < a} \\ \mathrm{J = 0} \quad \rightarrow \mathrm{B}_\theta = B_{\theta\, a} \dfrac{a}{r} & \mathrm{a < r \le b} \end{cases}, \qquad (9)$$

where $B_{\theta a} = \dfrac{\mu_0 I_p}{2\pi a}$.

Then first approximate value for the internal inductance can be easily obtained by substituting Eq. (9) in Eq. (8):

$$li_2 = \frac{1}{2} - 2\ln\frac{a}{b}, \qquad (10)$$

where this relation for IR-T1 tokamak parameters equal to value of 0.994.

Second approximate value for the internal inductance can be determined from the well-known Bennett current density profile, as:

$$\begin{cases} J = \dfrac{I_p}{\pi} \dfrac{a^2}{\left(r^2 + a^2\right)^2} & \mathrm{r \le a} \\ \mathrm{J = 0} & \mathrm{a < r < b} \end{cases}, \qquad (11)$$

therefore, the poloidal magnetic field profile can be obtained:

$$\begin{cases} B_\theta = \dfrac{\mu_0 I_p}{2\pi} \left[\dfrac{\mathrm{r}}{\mathrm{r}^2 + a^2} \right] & \mathrm{r \le a} \\ \mathrm{B}_\theta = \dfrac{\mu_0 I_p}{4\pi\ \mathrm{r}} & \mathrm{a < r < b} \end{cases}, \qquad (12)$$

and then second approximate value for internal inductance can be obtained:

$$li_3 = \frac{1}{2}\left(\ln\frac{4b}{a} - 1 \right), \qquad (13)$$

where this relation for IR-T1 tokamak parameters equal to value of 0.332.

In general case, for the large aspect ratio and circular plasma, the current density distribution is [2]:

$$\begin{cases} J = J(0)\left(1 - \dfrac{r^2}{a^2}\right)^{\upsilon} & \mathrm{r \le a} \\ J = 0 & \mathrm{a < r < b} \end{cases}, \qquad (14)$$

The poloidal magnetic field profile can be obtained:

$$\begin{cases} B_\theta = \dfrac{\mu_0 J(0) a^2}{2(\upsilon+1) r} \left(1 - \left(1 - \dfrac{r^2}{a^2} \right)^{\upsilon+1} \right), & \mathrm{r \le a} \\ B_\theta = \dfrac{\mu_0 J(0) a^2}{2(\upsilon+1) r} & \mathrm{a < r < b} \end{cases} \qquad (15)$$

where

$$\upsilon = \frac{q(a)}{q(0)} - 1 = \frac{\pi\, \mathrm{a}^2 J(0)}{I_P} - 1 \qquad (16)$$

If we assume a more peaked current profile with central safety factor $q(0) \approx 1$, then the fourth approximate values of the internal inductances can be determined from substituting the Eq. (15) in Eq. (8) as a function of the υ. Results present in table 2 and Figure (1).

Table 2. Dependence of the Internal Inductance to the values of υ for IR-T1 tokamak parameters

υ	**Internal Inductance (li_4)**	υ	**Internal Inductance (li_4)**
0	0.994	6	2.428
1	1.410	7	2.548
2	1.710	8	2.656
3	1.942	9	2.754
4	2.132	10	2.842
5	2.292	11	2.924

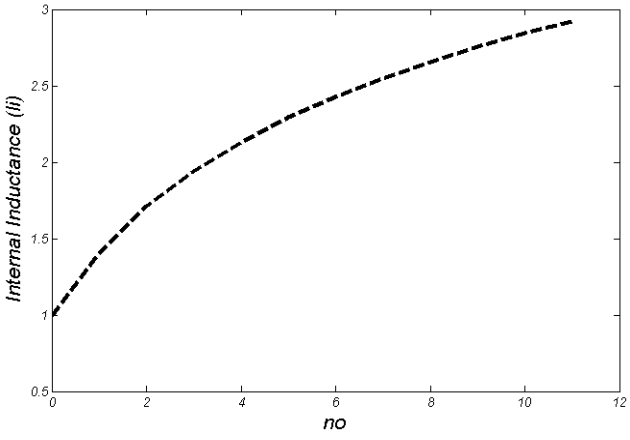

Figure (1). Dependence of the Internal Inductance to the values of υ for IR-T1 tokamak parameters

Our experiments show that the value of υ which proportional to the edge safety factor reduced from 8 to 1 along time interval of plasma current (see Figure (2)). Therefore, according to recent calculations for the IR-T1 tokamak plasma, the values of internal inductance reduced from 2.5 to 1.2 along the time interval of plasma current.

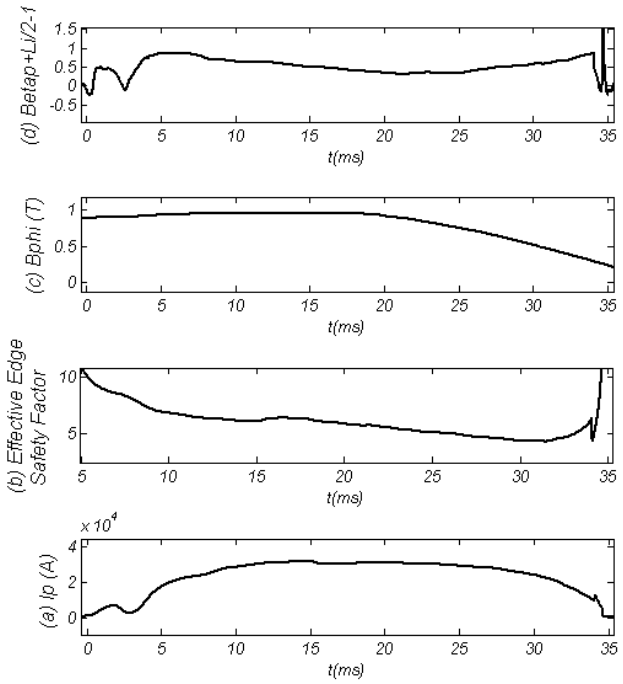

Figure (2). Combination of the Diamagnetic Loop and Magnetic Probe Results: (a) Plasma Current, (b) Effective Edge Safety Factor, (c) Toroidal Magnetic Field, and (d) Shafranov Parameter

4. Experimental Result for Measurement of the Plasma Internal Inductance

Table 3. Design parameters of the magnetic probe and diamagnetic loop

Parameters	Magnetic Probe	Diamagnetic Loop
R (Resistivity)	33 Ω	100 Ω
L (Inductance)	1.5mH	20mH
n (Turns)	500	170
S (Sensitivity)	0.7mV/G	0.5V/G
f (Frequency Response)	22kHz	5kHz
Effective nA	0.022 m^2	16 m^2
d (Wire Diameter)	0.1mm	0.2mm
d_m (Coil Average Radius)	3mm	175mm

According to experimental approach in section 2, In the IR-T1 tokamak an array of four magnetic probes were designed, two magnetic probes were installed on the circular contour Γ of the radius $b = 16.5cm$ in angles of $\theta = 0$ and $\theta = \pi$ to detect the tangential component of the magnetic field B_θ and two magnetic probes are also installed above, $\theta = \pi / 2$, and below, $\theta = 3\pi / 2$, to detect the normal component of the magnetic field B_ρ.

Also, a diamagnetic loop with its compensation coil were constructed, and installed on outer surface of the IR-T1 tokamak chamber, and then the poloidal beta measured from them. After measurements of $\langle B_\theta \rangle$ and $\langle B_\rho \rangle$, and then the Shafranov parameter from magnetic probes, I_p from rogowski coil, poloidal beta from diamagnetic loop and substituting them in to Eq. (4), the internal inductance was measured. Results presented in the Fig. (3). Design parameters of the magnetic pickup coils presented in Table 3. Diamagnetic loop and its compensating coil also were constructed and installed on the IR-T1 tokamak. Its characteristics are also shown in Table 3.

As shown in Figure (3), the values of the internal inductance reduced from 2 to 0.61 along the time internal of the plasma current.

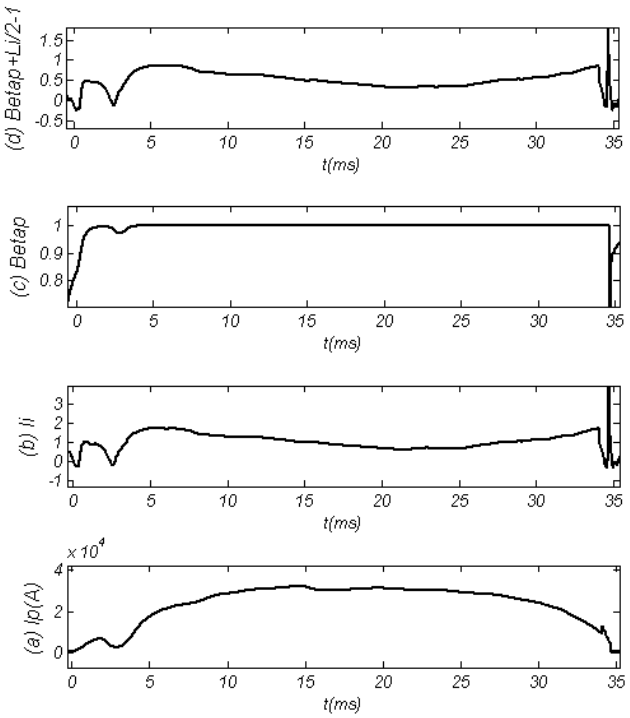

Figure (3). Combination of the Diamagnetic Loop and Magnetic Probe Results: (a) Plasma Current, (b) Internal Inductance obtained by Subtraction of Poloidal Beta (c), from Shafranov Parameter (d). As observable, the internal inductance reduces from 2 to 0.61

5. Summary

Array of magnetic probes and also a diamagnetic loop with its compensation coil have been designed, constructed, and installed on outer surface of the IR-T1 tokamak chamber. The poloidal and radial components of the magnetic fields and also diamagnetic flux signal measured, and therefore the Shafranov parameter and poloidal beta and then the plasma internal inductance were measured from them. Also, a few approximate values of the internal inductance calculated.

ACKNOWLEDGEMENTS

This work was supported by Shabestar-Branch, Islamic Azad University, under contract number 51953911010006.

REFERENCES

[1] V. S. Mukhovatov and V. D. Shafranov: Nucl. Fusion 11, (1971), 605.

[2] J. Wesson, Tokamaks, Clarendon, Oxford, 1997, pp. 105–131.

[3] E. J. Strait and et al., 2006, Fusion Science and Technology, 53, pp. 304-330.

[4] M. Spolaore et al., Czech. J. Phys. 55 (12), 1615-1621, (2005).

[5] P. Devynck et al., Physics of Plasmas 13 (10), 102505-102513, (2006).

[6] A. Salar Elahi et al., IEEE Trans. Plasma Science, 40, 892-897, (2012).

[7] B. Viatcheslav et al., J. Plasma Fusion Res. 5, 418-423, (2002).

[8] E. Y. Wang et al., Nucl. Fusion 35, 467, (1995).

[9] Ch. P. Ritz et al., Rev. Sci. Instrum. 59, 1739-1744, (1998).

[10] V. V. Bulanin et al., Plasma Phys. Control. Fusion 48, A101, (2006).

[11] J. A. C. Cabral et al., Plasma Phys. Control. Fusion 40, 1001, (1998).

[12] C. Silva et al., 17th IAEA Fusion Energy Conference, EX/P1-10 Lyon, France, (2002)

[13] A. Salar Elahi et al., IEEE Trans. Plasma Science 38 (2), 181-185, (2010).

[14] A. Salar Elahi et al., IEEE Trans. Plasma Science 38 (9), 3163-3167, (2010).

[15] M. Emami, M. Ghoranneviss, A. Salar Elahi and A. Rahimi Rad, J. Plasma Phys. 76 (1), 1-8, (2009).

[16] A. Salar Elahi et al., Fusion Engineering and Design 85, 724–727, (2010).

[17] A. Salar Elahi et al., Phys. Scripta 80, 045501, (2009).

[18] A. Salar Elahi et al., Phys. Scripta 80, 055502, (2009).

[19] A. Salar Elahi et al., Phys. Scripta 81 (5), 055501, (2010).

[20] A. Salar Elahi et al., Phys. Scripta 82, 025502, (2010).

[21] M. Ghoranneviss, A. Salar Elahi et al., Phys. Scripta 82 (3), 035502, (2010).

[22] A. Salar Elahi et al., J. Fusion Energy 28 (4), 346-349, (2009).

[23] A. Salar Elahi et al., J. Fusion Energy 28 (4), 416-419, (2009).

[24] A. Salar Elahi et al., J. Fusion Energy 28 (4), 408-411, (2009).

[25] A. Salar Elahi et al., J. Fusion Energy 28 (4), 412-415, (2009).

[26] A. Salar Elahi et al., J. Fusion Energy 28 (4), 394-397, (2009).

[27] A. Salar Elahi et al., J. Fusion Energy 28 (4), 404-407, (2009).

[28] A. Salar Elahi et al., J. Fusion Energy 28 (4), 390-393, (2009).

[29] A. Salar Elahi et al., J. Fusion Energy 28 (4), 385-389, (2009).

[30] A. Rahimi Rad, M. Ghoranneviss, M. Emami, and A. Salar Elahi, J. Fusion Energy 28 (4), 420-426, (2009).

[31] A. Salar Elahi et al., J. Fusion Energy 29 (1), 1-4, (2010).

[32] A. Salar Elahi et al., J. Fusion Energy 29 (1), 22-25, (2010).

[33] A. Salar Elahi et al., J. Fusion Energy 29 (1), 29-31, (2010).

[34] A. Salar Elahi et al., J. Fusion Energy 29 (1), 26-28, (2010).

[35] A. Salar Elahi et al., J. Fusion Energy 29 (1), 32-35, (2010).

[36] A. Salar Elahi et al., J. Fusion Energy 29 (1), 36-40, (2010).

[37] A. Salar Elahi et al., J. Fusion Energy 29 (1), 62-64, (2010).

[38] A. Salar Elahi et al., J. Fusion Energy 29 (1), 76-82, (2010).

[39] A. Rahimi Rad, M. Emami, M. Ghoranneviss, A. Salar Elahi, J. Fusion Energy 29 (1), 73-75, (2010).

[40] A. Salar Elahi et al., J. Fusion Energy 29 (1), 83-87, (2010).

[41] A. Salar Elahi et al., J. Fusion Energy 29 (1), 88-93, (2010).

[42] A. Salar Elahi et al., J. Fusion Energy 29 (3), 209-214, (2010).

[43] A. Salar Elahi et al., J. Fusion Energy 29 (3), 232-236, (2010).

[44] A. Salar Elahi et al., J. Fusion Energy 29 (3), 251-255, (2010).

[45] A. Salar Elahi et al., J. Fusion Energy 29 (3), 279-284, (2010).

[46] M. Ghoranneviss, A. Salar Elahi et al., J. Fusion Energy 29 (5), 467-470, (2010).

[47] A. Salar Elahi et al., J. Fusion Energy 29 (5), 461-465, (2010).

[48] A. Salar Elahi et al., Brazilian J. Physics 40 (3), 323-326, (2010).

[49] A. Salar Elahi et al., J. Fusion Energy 30 (2), 116-120, (2011).

[50] M.R. Ghanbari, M. Ghoranneviss, A. Salar Elahi et al., Phys. Scripta 83, 055501, (2011).

[51] A. Salar Elahi, J. Fusion Energy 30 (6), 477-480, 477-480, (2011).

[52] A. Salar Elahi et al., Fusion Engineering and Design 86, 442–445, (2011).

[53] A. Salar Elahi et al., J. Fusion Energy 31 (2), 191-194, (2012).

[54] M.R. Ghanbari, M. Ghoranneviss, A. Salar Elahi and S. Mohammadi, Radiation Effects & Defects in Solids 166 (10), 789–794, (2011).

[55] A. Salar Elahi et al., IEEE Trans. Plasma Science (January 2013, in press), DOI: 10.1109/TPS.2012.2235186.

[56] A. Salar Elahi et al., Accepted for publication in Radiation Effects & Defects in Solids (January 2012, in press), DOI: 10.1080/10420150.2011.650171.

[57] Z. Goodarzi, M. Ghoranneviss and A. Salar Elahi, Accepted for the publication in J. Fusion Energy (March 2012, in press), DOI: 10.1007/s10894-012-9526-4.

[58] M.R. Ghanbari, M. Ghoranneviss, A. Salar Elahi et al., Phys. Scripta 85 (5), 055502, (2012).

[59] A. Salar Elahi et al., Accepted for the publication in Radiation Effects and Defects in Solids (June 2012, in press), DOI: 10.1080/10420150.2012.706609.

[60] A. Salar Elahi et al., Accepted for the publication in Radiation Effects and Defects in Solids (June 2012, in press), DOI: 10.1080/10420150.2012.706607.

[61] K. Mikaili Agah, M. Ghoranneviss, A. Salar Elahi et al., accepted for the publication in J. Fusion Energy (July 2012, in press), DOI: 10.1007/s10894-012-9563-z.

[62] A. Salar Elahi et al., J. Nuclear and Particle Physics 1(1), (2011), 10-15, DOI: 10.5923/j.jnpp.20110101.03.

[63] A. Salar Elahi et al., J. Nuclear and Particle Physics 2(2), (2012), 1-5, DOI: 10.5923/j.jnpp.20120202.01.

[64] A. Salar Elahi et al., Fusion Engineering and Design (January 2013, in press), DOI: 10.1016/j.fusengdes. 2012.12.001.

[65] A. Salar Elahi et al., J. Nuclear and Particle Physics 2(2), 22-25, (2012), DOI: DOI: 10.5923/j.jnpp.20120202.05.

[66] A. Salar Elahi et al., J. Nuclear and Particle Physics 2(5), 112-118, (2012), DOI: 10.5923/j.jnpp.20120205.02.

[67] A. Salar Elahi et al., J. Nuclear and Particle Physics 2(6), 142-146, (2012), DOI: 10.5923/j.jnpp.20120206.02.